

# Momentum roughness and zero-plane displacement of ridge-furrow tilled soil\*

K.J. McInnes, J.L. Heilman and R.W. Gesch

*Department of Soil and Crop Sciences, Texas A&M University, College Station, TX 77843, USA*

(Received 7 August 1990; revision accepted 6 October 1990)

## ABSTRACT

McInnes, K.J., Heilman, J.L. and Gesch, R.W., 1991. Momentum roughness and zero-plane displacement of ridge-furrow tilled soil. *Agric. For. Meteorol.*, 55: 167–179.

Estimation of heat and mass transfer between the atmosphere and the ground surface by flux-profile relationships may be influenced by the values chosen for zero-plane displacement  $d$  and momentum roughness  $z_{0m}$ . This study was conducted to determine the effect of wind direction on  $d$  and  $z_{0m}$  of a ridge–furrow tilled soil. Fifteen-minute average wind-speed and air-temperature profiles, together with wind direction, measured over a 28-day period above a ridge–furrow tilled field near College Station, TX, were used to determine  $d$  and  $z_{0m}$  as a function of wind direction relative to ridge orientation. The difference in height  $h$  between the ridge tops and furrow bottoms was 0.22 m and the spacing between ridges was 1 m. A trade-off between  $d$  and  $z_{0m}$  that did not appreciably alter the fit of theoretical to measured wind-speed profiles made separation of  $d$  and  $z_{0m}$  difficult. No strong relationship was found between  $d$  or  $z_{0m}$  and wind direction when both were allowed to vary and the best fits of theoretical to measured wind-speed profiles were found by a least sum of error squares technique. When  $z_{0m}$  was held constant and  $d$  allowed to vary, the best overall fit was with  $z_{0m}/h=0.032$  and  $d/h$  varying from about 0.091 to 1.2 when the wind direction was parallel and perpendicular to the ridges, respectively. When  $d$  was held constant and  $z_{0m}$  allowed to vary, the best overall fit was with  $d/h=0.85$  and  $z_{0m}/h$  varying from 0.011 to 0.055 when the wind direction was parallel and perpendicular to the ridges, respectively. The implication to estimation of heat or mass transport between the atmosphere and the surface of a ridge-furrow tilled soil where  $d$  and  $z_{0m}$  are required in the calculations is that wind direction should be considered.

## INTRODUCTION

Cultivation that leaves ridges and furrows of some form is widely practised throughout the world. There is a need to predict the vertical fluxes of heat and mass from the soil surface to the atmosphere in many of these areas. Calculations of these fluxes based on flux–profile relationships are influenced, in

---

\*Technical Article TA-25771 from the Texas Agricultural Experiment Station, College Station, TX 77843, USA.

part, by the values chosen for the displacement height  $d$  and momentum roughness  $z_{0m}$  which determine the shape of the wind-speed profiles. For example, the equation describing the aerodynamic resistance to transfer of momentum between the soil surface and a given height, a resistance often equated to that for heat and mass transport, contains both  $d$  and  $z_{0m}$  (Monteith and Unsworth, 1990). The effective aerodynamic characteristics of ridge-furrow tilled soil change with the angle the wind makes with respect to the direction of the cultivation and both  $d$  and  $z_{0m}$  are probably affected by wind direction. When the wind blows perpendicular to the ridges, the ridges along with soil clods may act as bluff bodies. When the wind is parallel, instead of acting as bluff bodies, the ridges may simply displace the profile above that for a flat surface.

Studies to relate  $d$  or  $z_{0m}$  to the height  $h$  of the roughness elements on the surface have met with limited success. For crop-covered surfaces the ratio  $z_{0m}/h$  has been found to be about 0.13 (Paeschke, 1937; Tanner and Pelton, 1960) while the ratio  $d/h$  has been reported to be about 0.64 (Cowan, 1968; Stanhill, 1969). Chamberlain (1968) estimated the ratio  $z_{0m}/h$  from wave-like roughness elements, with the wind perpendicular to the elements, to range from 0.07 to 0.12, depending on the height and spacing  $l$  of the elements. A value of 0.4 for the ratio  $d/h$  was reported for one arrangement with  $h/l=0.1$ . Rider (1957) reported values of the ratio  $d/h$  ranging from 0.4 to 0.6 for ridge-furrow tilled soil, but gave no information on the direction of the wind in the study or possible effect of wind direction. Other formulations involving more characteristics of the roughness elements have been derived for  $d$  and  $z_{0m}$  over surfaces with bluff obstacles (Lettau, 1969; Wooding et al., 1973); however, the accuracy of these formulations is low, and there is still no good substitute for the experimental determination of the parameters by wind-speed profile analysis (Brutsaert, 1982).

The purpose of this experiment was to determine, from wind-speed profile analysis, the effect of wind direction on  $d$  and  $z_{0m}$  of a ridge-furrow tilled field.

## MATERIALS AND METHODS

### *Field measurements*

Cup anemometers (Model 12102D, R.M. Young Co., Traverse City, MI)<sup>a</sup> and ceramic wick thermocouple psychrometers (Gay, 1972) were installed for profile measurements in the center of a 25-ha ridge-furrow tilled field near College Station, TX, from November 11 through December 8, 1989. The sensors were located 0.40, 0.52, 0.67, 0.86, 1.11, 1.44, 1.86 and 2.40 m above

<sup>a</sup>Trade names and company names are included for the benefit of the reader. No endorsement is implied.

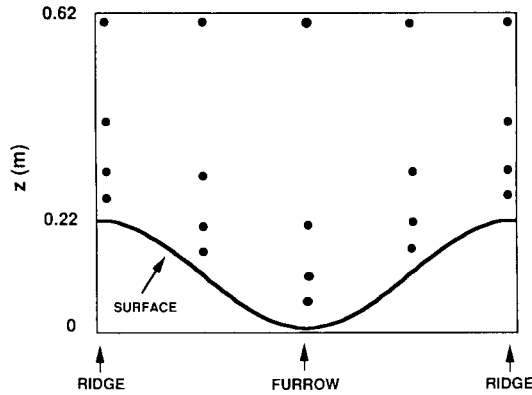


Fig. 1. Locations of heat-transport anemometers.

the tops of the ridges. The difference in height  $h$  between the ridge top and furrow bottom was 0.22 m and the spacing between ridges was 1 m. The ridges were oriented  $26^\circ$  E of N and minimum fetch was in excess of 230 m in all directions. Average wind speeds, dry- and wet-bulb air temperatures, and  $5^\circ$ -bin wind-direction frequency were recorded every 15 min, with a model CR7X data logger (Campbell Scientific, Logan, UT)<sup>a</sup>. Average wind directions were calculated from the wind-direction frequencies.

In addition to the above measurements, wind speeds were measured between and up to 0.40 m above the furrows with an array of 20 heat-transport anemometers constructed in our lab after the design of Kanemasu and Tanner (1968). Anemometers were placed above the ground surface as shown in Fig. 1.

#### Determination of $d$ and $z_{0m}$

The method for determining  $d$  and  $z_{0m}$  was by minimizing the sum of squares of error  $ss_e$  between measured and theoretical wind speeds. In the surface sublayer, the sum of squares of the error between  $n$  theoretical and measured mean wind speeds may be expressed as

$$ss_e \sum_{i=1}^n (u_i - (u_*/k) \{ \ln[(z_i - d)/z_{0m}] + \Psi_m \})^2 \quad (1)$$

where  $u_i$  is the measured wind speed at height  $z_i$ ,  $u_*$  is the friction velocity,  $k$  is von Karman's constant, and  $\Psi_m$  is a correction for atmospheric stability. To determine  $ss_e$  with given  $d$  and  $z_{0m}$  values,  $\Psi_m$  must be known. For unstable conditions we used the formulations given by Businger (1975):

$$\Psi_m = 2 \ln[(1+x)/2] + \ln[(1+x^2)/2] - 2 \arctan(x) + \pi/2 \quad (2)$$

$$x = \phi_m^{-1} \quad (3)$$

$$\phi_m = [1 - 16(z-d)/L]^{-0.25} \quad (4)$$

$$L = -\rho c_p T u_*^3 / (g H k) \quad (5)$$

$$H = [\rho c_p k (z-d) u_* / \phi_h] \partial T / \partial z \quad (6)$$

$$\phi_h = [1 - 16(z-d)/L]^{-0.5} \quad (7)$$

$$u_* = (1/n) \sum_{i=1}^n (u_i k / \{\ln[(z_i - d)/z_{0m}] + \Psi_m\}) \quad (8)$$

Here,  $L$  is the Monin–Obukov scaling length,  $g$  is the acceleration due to gravity,  $H$  is the sensible heat flux,  $T$  is the potential air temperature, and  $\rho c_p$  is the volumetric heat capacity of air. Equations (2)–(8) were solved iteratively to determine  $L$  and calculate a value of  $\Psi_m$  that was then used to correct the theoretical mean-wind profile in eqn. 1 for instability. In this study,  $z$  was referenced to the bottom of the furrow.

For stable conditions we used the same procedure as above except we substituted the formulation of  $\phi_m$  (Thom, 1975), derived with the Richardson number  $Ri$

$$\phi_m = \phi_h = (1 - 5Ri)^{-1} \quad (9)$$

where

$$Ri = (g/T) (\partial T / \partial z) / (\partial u / \partial z)^2 \quad (10)$$

but kept  $\Psi_m$  as a function of  $L$  (Businger, 1975)

$$\Psi_m = 4.7(z-d)/L \quad (11)$$

The reason for using the formulation of  $\phi_m$  with  $Ri$  as the argument and not  $L$  is that the iteration to find  $\Psi_m$  does not converge for stable conditions when  $\phi_m = \phi_h = (1 + 4.7(z-d)/L)$ . The air-temperature gradient used in calculating  $Ri$  and  $H$ , and  $\partial u / \partial z$  used in calculating  $Ri$  were determined from the slopes of power functions of temperature and mean wind speed with height, respectively.

Several approaches to finding the minimum  $ss_e$  as a function of both  $d$  and  $z_{0m}$  exist. Stearns (1970) simultaneously solved  $\partial ss_e / \partial d = 0$  and  $\partial ss_e / \partial z_{0m} = 0$  for  $d$  and  $z_{0m}$ . We chose instead three approaches that searched the  $d$ - $z_{0m}$ - $ss_e$  surface for the minimum  $ss_e$  value. In the first procedure, a rectangular grid of  $ss_e$  values for combinations of  $z_{0m}$  and  $d$  was produced, and then the combination producing the minimum  $ss_e$  was found from this matrix. Second, values of  $z_{0m}$  were determined for  $d$  values from 0 to 0.5 m by 0.01-m increments, and third,  $d$  values were determined for  $z_{0m}$  values from 1 to 50 mm by 1-mm increments. When either  $d$  or  $z_{0m}$  was set constant in these latter two procedures, the value of the other that gave the minimum  $ss_e$  was determined

by the golden-section search technique (Shoup, 1979). The reasons for these latter two procedures will be discussed later. For all three procedures, only profiles where the average wind speed at 0.40 m above the ridge top was greater than  $1.0 \text{ m s}^{-1}$  were used. The total number of profiles used was 1859. Limits on the values of  $d$  and  $z_{0m}$  used in the golden-section search were  $0 \leq d < 0.62 \text{ m}$  and  $0.001 \leq z_{0m} \leq 220 \text{ mm}$ , respectively.

## RESULTS AND DISCUSSION

As pointed out by Stearns (1970) and shown here in Fig. 2, the surface defined by a matrix consisting of the  $ss_e$  between theoretical and measured wind-speed profiles with combinations of  $z_{0m}$  and  $d$  shows a trough with a base that has little relief along a  $d$ - $z_{0m}$  curve. Figure 3A shows a contour plot of  $ss_e$  derived with a hypothetically measured wind-speed profile defined for the eight sample heights used in this experiment and with  $d=0.1 \text{ m}$ ,  $u_* = 0.3 \text{ m s}^{-1}$ ,  $z_{0m}=0.01 \text{ m}$  and  $\Psi_m=0$ . Overlain on this contour plot are the corresponding values of  $u_*$ . Although we have clipped Fig. 3, note from Fig. 2, which was derived with the same parameters, that the trough extends to  $d > 0.22 \text{ m}$ , the height of the ridges in this study, and would have extended to  $d < 0 \text{ m}$  had we not set the limit  $d \geq 0 \text{ m}$ . A plot of  $d$  against  $z_{0m}$  for the best fits to the profiles where  $d < 0.22 \text{ m}$  is given in Fig. 3B. If overlain on Fig. 3A, most of the points in Fig. 3B fall within the first contour level. This is in part because the values of  $d$  and  $z_{0m}$  chosen for the profile from which Fig. 3A was generated were in the ranges of realistic values for this surface. Values of  $d > 0.22 \text{ m}$  giving the best fit were commonly obtained and along with the

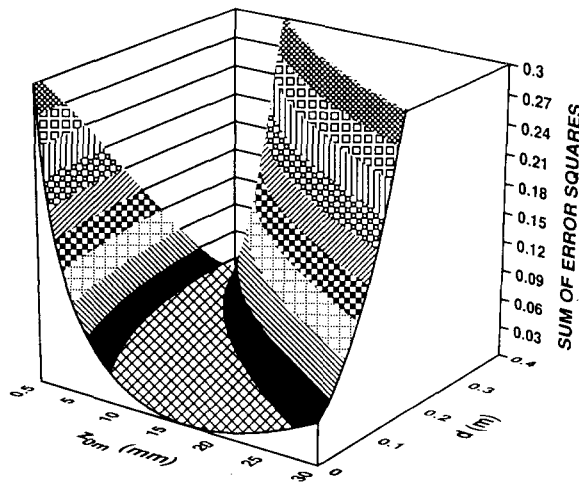


Fig. 2. Typical  $d$ - $z_{0m}$ - $ss_e$  surface for this study. The surface shown is for  $ss_e \leq 0.3 \text{ m}^2 \text{ s}^{-2}$ .

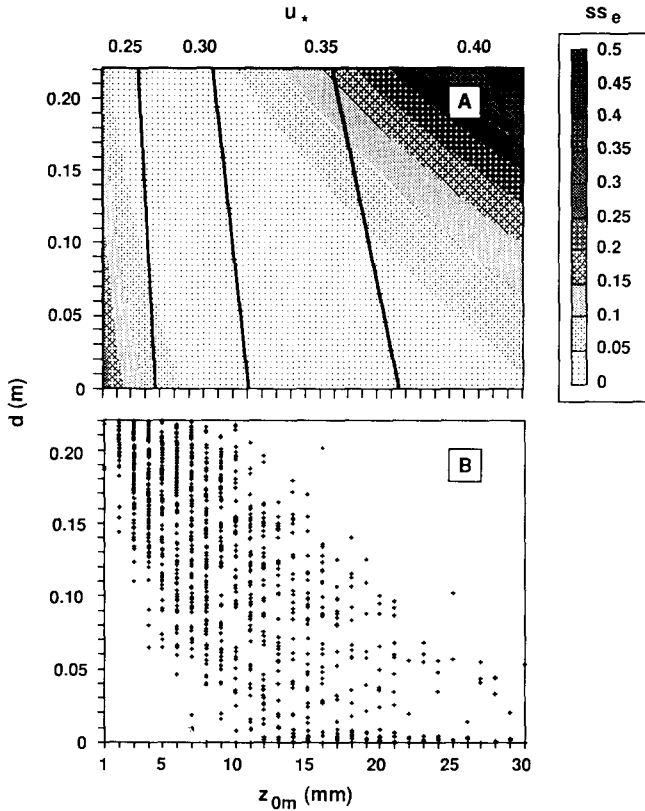


Fig. 3. Contour plot of  $ss_e$  between wind-speed profiles defined with combinations of  $z_{0m}$  and  $d$  and a profile defined by  $z_{0m}=10$  mm,  $d=0.1$  m and  $u_* = 0.3$  m s<sup>-1</sup> (A). Relationship between  $d$  and  $z_{0m}$  from least error squares fitted wind-speed profiles (B).

corresponding value of  $z_{0m}$  produced an  $ss_e$  that generally fell within the first contour level of Fig. 3A.

From the trough in Fig. 2, it was evident that different combinations of  $d$ ,  $u_*$  and  $z_{0m}$  gave nearly equivalent fits to wind profile data. We determined the relationships between  $d$  and  $z_{0m}$  from combinations of the two parameters that produced the least  $ss_e$  using the eight heights mentioned above while allowing  $u_*$  to vary and trading  $d$  for  $z_{0m}$  (Fig. 4). On this figure, vertical lines from a given  $z_{0m}$  intersect the curves at  $d$  values producing perfect fit. Horizontal lines from a given  $d$  intersect the curves at  $z_{0m}$  values producing perfect fit. Other combinations of  $d$  and  $z_{0m}$  falling on the same curve represent values giving the least  $ss_e$  fit to the profile of best fit when either  $d$  or  $z_{0m}$  is changed. These curves are valid for combinations of  $d$  and  $z_{0m}$  when measurements are taken at the same sample heights as mentioned above. Curves similar to these could have been used to explain the diurnal variation in  $d$  and  $z_{0m}$  found by Pieri and Fuchs (1990) for a wide-row-spaced cotton crop. These

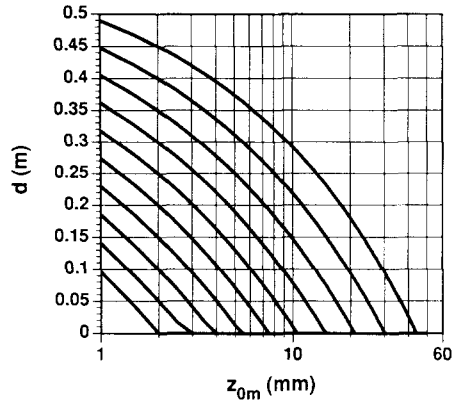


Fig. 4. Least  $ss_e$  trade-off curves for  $d$  and  $z_{0m}$ .

trade-off curves may be the same for different profiles. Profiles defined from the combination of  $d=0.4$  m and  $z_{0m}=2$  mm, for example, share the same curve as profiles from the combination of  $d=0$  m and  $z_{0m}=30$  mm. The points of best fit on the curve for different combinations, though, are obviously not the same. In practice, because the theoretical wind speeds in eqn. 1 are not an exact description of real wind speeds and because of experimental error, the point of best fit on the curve may not be as well defined as it is in theory. The friction velocity  $u_*$  associated with these curves increases as  $d$  decreases or  $z_{0m}$  increases (Fig. 3A). An independent measure of  $u_*$  may aid the choice of the best combination of  $d$  and  $z_{0m}$ . However, if  $\pm 10\%$  were a reasonable degree of accuracy for measurements of  $u_*$ , there would still be considerable uncertainty in  $d$  and  $z_{0m}$  (Fig. 3A).

The relationships between  $z_{0m}$  and wind direction and  $d$  and wind direction that resulted from our first procedure were not well defined (Fig. 5). An increase in  $z_{0m}$  as the wind shifted from parallel to perpendicular to the ridges is shown, but there was much scatter. Because we felt much of this scatter was the result of the trade-off between  $d$  and  $z_{0m}$ , we chose then to follow the second and third procedures to determine the effect of wind direction on  $d$  and  $z_{0m}$ . In the second procedure, we determined the value of  $z_{0m}$  that gave the best overall fit to the profiles, then held it constant and found how  $d$  varied with wind direction. Here, overall implies the sum of the  $ss_e$  for all 1859 profiles. The value of  $z_{0m}$  that gave the best overall fit was 7 mm (Fig. 6). The overall  $ss_e$  when  $z_{0m}=7$  mm was  $10.5 \text{ m}^2 \text{ s}^{-2}$ , about 27% greater than the total of  $8.3 \text{ m}^2 \text{ s}^{-2}$  for the combinations of  $d$  and  $z_{0m}$  giving the best fits. Considering there were 1859 profiles overall, the difference of  $2.2 \text{ m}^2 \text{ s}^{-2}$  in fit produced an added error that was well beyond the accuracy of our anemometers. Values of  $d$  at wind directions perpendicular to the ridges exceeded the heights

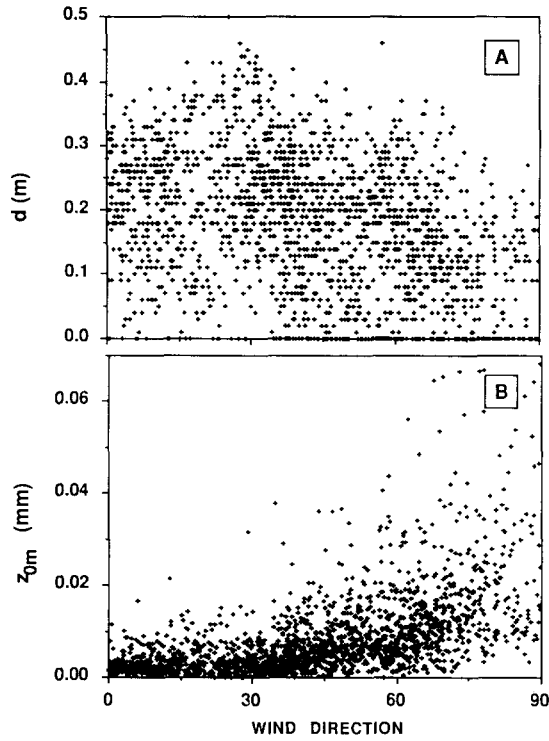


Fig. 5. Relationships between  $d$  and wind direction (A) and  $z_{0m}$  and wind direction (B) from least squares fitted wind-speed profiles. Wind directions  $0^\circ$  and  $90^\circ$  are parallel and perpendicular to the direction of the ridges, respectively.

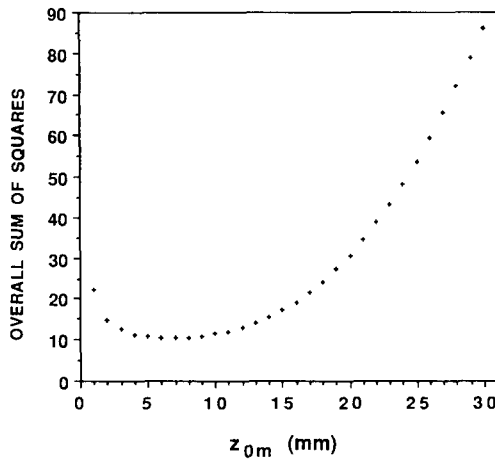


Fig. 6. Relationship between overall  $ss_e$  and  $z_{0m}$  for all profiles measured.

of the ridges by about 0.04 m ( $d/h=1.2$ ) (Fig. 7). Values of  $d$  when the wind was parallel to the ridges were about 0.02 m ( $d/h=0.091$ ).

If values of  $d$  were to be restricted to being  $\leq h$ , then that fraction of  $d$  that would have been 0.22 m must be accounted for by a corresponding increase in  $z_{0m}$  (Fig. 4). For example, a value of  $z_{0m}=10$  mm for all profiles gave values of  $d$  that were about equal to the height of the ridges when the wind was perpendicular to the rows and only increased overall  $ss_e$  by  $0.9 \text{ m}^2 \text{ s}^{-2}$ . When this value of  $z_{0m}$  was chosen,  $d$  varied from near 0 m when the wind blew parallel to the ridges to the height of the ridges when the wind blew perpendicular.

Our computer-generated contour map of the wind in and around the furrow and ridges measured with the heat-transport anemometers (Fig. 8) suggests that a value of  $d > h$  may be warranted. In the wake of the furrow, an eddy extending above  $h$  formed when the wind was perpendicular to the ridge direction. This is consistent with Businger's (1975) analysis of wind profiles over shelter belts. When the wind flowed parallel to the ridges, the wind was horizontally uniform at a much lower height above the ridge tops than it was when the wind blew perpendicular. A value of  $d=0$  m when  $z$  is referenced to the bottom of the furrow is probably more objectionable than values of  $d > h$ , since the ridges must displace the profile compared with a flat surface with the same roughness elements.

Our third approach was to find the value of  $d$  that gave the best overall fit to the data, hold it constant, and determine how  $z_{0m}$  varied with wind direction. The value of  $d$  that gave the best fit was 0.18 m (Fig. 9). The least overall  $ss_e$  with  $d$  constant was 12% greater than the total for the combinations of  $z_{0m}$  and  $d$  giving the best fits. The overall  $ss_e$  with  $d=0$  m or  $d=h$  was not much greater than that with  $d=0.18$  m. With  $d=0.18$  m,  $z_{0m}$  varied from about 2.5 to 12 mm ( $z_{0m}/h$  from 0.011 to 0.055) when the wind was parallel and per-

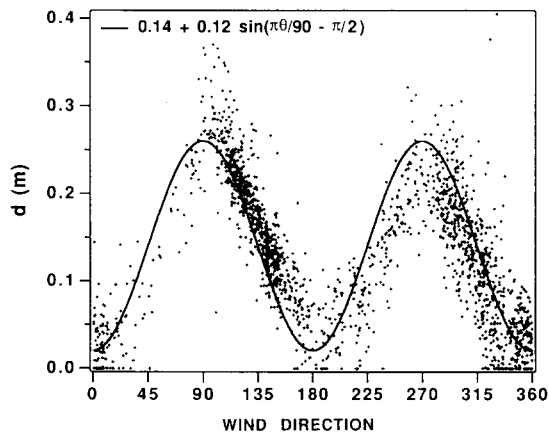


Fig. 7. Relationship between  $d$  and wind direction  $\theta$  for  $z_{0m}=7$  mm. Wind directions 0, 180 and 360° are parallel to the ridges and 90 and 270° are perpendicular.

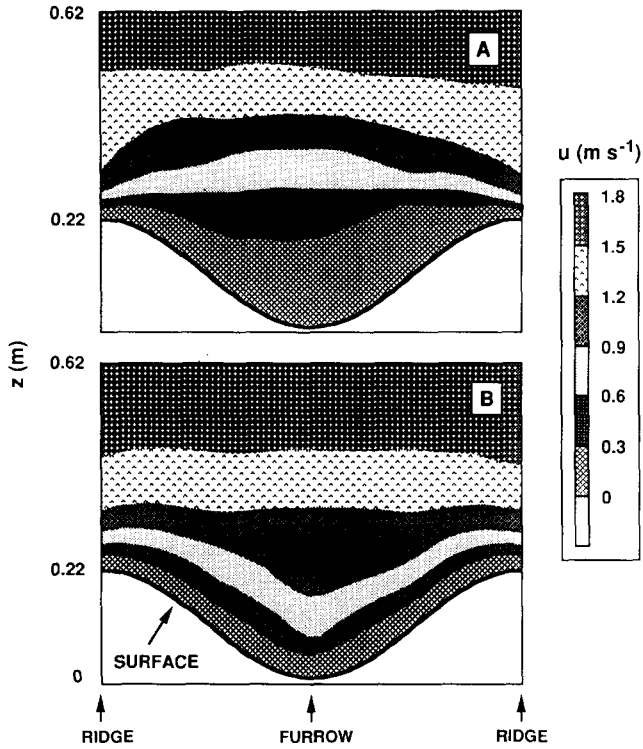


Fig. 8. Contour plots of the wind speed near the surface of ridge-furrow tilled soil when the wind direction was perpendicular (A) and parallel (B) to the ridge direction. In A the wind was from right to left. The wind speeds at  $z=0.62$  m for A and B were  $1.6$  and  $1.7$   $\text{m s}^{-1}$ , respectively.

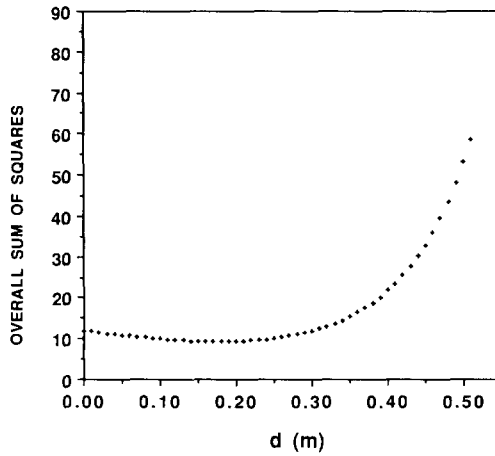


Fig. 9. Relationship between overall  $ss_e$  and  $d$  for all profiles measured.

pendicular to the rows, respectively (Fig. 10). Figure 10 may also be derived from either Fig. 5 or Fig. 7 using the trade-off curves. For example, from Fig. 7 when  $z_{0m} = 7$  mm,  $d$  ranged from about 0.02 to 0.26 m when the wind was parallel and perpendicular to the ridge direction, respectively. If it were desired to find how  $z_{0m}$  varied when  $d = 0.18$  m, the curves containing the intersections of  $z_{0m} = 7$  mm with  $d = 0.02$  m and  $d = 0.26$  m must be located on Fig. 4. Next, the  $z_{0m}$  values intersecting these curves at  $d = 0.18$  m must be found. Visual estimation with this procedure produced  $z_{0m}$  values of about 2.5 mm when the wind was parallel to the ridges and 12 mm when the wind was perpendicular. The solid line in Fig. 10 shows the directional variation in the  $d$  sine wave in Fig. 7 transformed into variation in  $z_{0m}$  with the above procedure.

The implication of these results, to estimation of heat and mass transport between the atmosphere and the surface of a ridge-furrow tilled soil when estimates of  $d$  and  $z_{0m}$  are needed, is that wind direction should be considered. The same may be true for estimates of heat and mass transport when wide-row-spaced crops are considered. For example, the adiabatic aerodynamic resistance to momentum transfer  $r_m$ , that is often used as a substitution for the resistances to heat and mass transfer, between the height  $d + z_{0m}$  and some reference height  $z$  with wind speed  $u$  is  $r_m = \ln[(z - d)/z_{0m}]^2 (k^2 u)$ . When  $z_{0m} = 7$  mm and  $z = 2$  m, the  $r_m$  that would be calculated when the wind direction is parallel to the ridges is 5% higher than the value when the wind is perpendicular. On the other hand, when  $d = 0.18$  and  $z_{0m}$  varies,  $r_m$  when the wind direction is parallel to the ridges is 72% higher than the value when the wind is perpendicular. From our data we cannot suggest which method is better. If one were to opt for holding  $z_{0m}$  constant and allowing  $d$  to vary so that  $r_m$  remained nearly constant, the rather large and directionally dependent val-

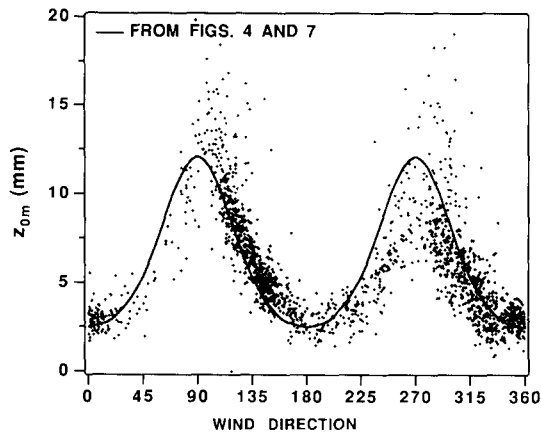


Fig. 10. Relationship between  $z_{0m}$  and wind direction for  $d = 0.18$  m. Solid line was estimated from the sine wave in Fig. 7 and the trade-off curves in Fig. 4.

ues of  $d$  would make estimation of a surface (height  $d + z_{0m}$ ) temperature or gas density for the calculation of fluxes difficult.

## CONCLUSIONS

Both  $d$  and  $z_{0m}$  of ridge-furrow tilled soil probably vary with wind direction; however, because the trade-off between the two parameters does not radically alter the least error squares fit to the data, separating them in this study was not possible because of a lack of an independent measure of  $u_*$ . Even with an independent measurement of  $u_*$ , separation may have been difficult. When  $d$  was held constant and  $z_{0m}$  allowed to vary with wind direction the overall fit to the data was better than when  $z_{0m}$  was held constant and  $d$  allowed to vary. Estimates of  $r_m$  varied more with wind direction when  $d$  was held constant and  $z_{0m}$  was allowed to vary than when  $z_{0m}$  was held constant and  $d$  allowed to vary. Detailed studies to determine the roughness lengths and displacement heights for heat and mass are needed if estimates of fluxes from ridge-furrow tilled soil using an aerodynamic resistance are to be performed.

## REFERENCES

- Brutsaert, W., 1982. *Evaporation into the Atmosphere: Theory, History, and Application*. D. Reidel, Dordrecht, 299 pp.
- Businger, J.A., 1975. Aerodynamics of vegetated surfaces. In: D.A. de Vries and N.H. Afgan (Editors), *Heat and Mass Transfer in the Biosphere*. Wiley, New York, pp. 139-165.
- Chamberlain, A.C., 1968. Transport of gases to and from surfaces with bluff and wave-like roughness elements. *Q. J. R. Meteorol. Soc.*, 94: 318-332.
- Cowan, I.R., 1968. Mass, heat and momentum exchange between stands of plants and their atmospheric environment. *Q. J. R. Meteorol. Soc.*, 94: 523-544.
- Gay, L.W., 1972. On the construction and use of ceramic wick thermocouple psychrometers. In: R.W. Brown and B.P. van Haveren (Editors), *Psychrometry in Water Relations Research*. Utah Agricultural Experiment Station, Utah State University, Logan, UT, pp. 251-258.
- Kanemasu, E.T. and Tanner, C.B., 1968. A note on a heat transport anemometer. *BioScience* 18: 327-329.
- Lettau, H., 1969. Note on aerodynamic roughness-parameter estimation on the basis of roughness element description. *J. Appl. Meteorol.*, 8: 828-832.
- Monteith, J.L. and Unsworth, M.H., 1990. *Principles of Environmental Physics*. Edward Arnold, New York, 291 pp.
- Paeschke, W., 1937. Experimentelle Untersuchungen zum Rauigkeits- und Stabilitätsproblem in der bodennahen Luftschicht. *Beitr. Freien Atmos.*, 24: 163-189.
- Pieri, P. and Fuchs, M., 1990. Comparison of Bowen ratio and aerodynamic estimates of evapotranspiration. *Agric. For. Meteorol.*, 49: 243-256.
- Rider, N.E., 1957. Water loss from various land surfaces. *Q. J. R. Meteorol. Soc.*, 83: 181-193.
- Shoup, T.E., 1979. *A Practical Guide to Computer Methods for Engineers*. Prentice Hall, Englewood Cliffs, NJ, 255 pp.

- Stanhill, G., 1969. A simple instrument for the field measurement of turbulent diffusion flux. *J. Appl. Meteorol.*, 8: 509–513.
- Stearns, C.R., 1970. Determining surface roughness and displacement height. *Boundary-Layer Meteorol.*, 1: 102–111.
- Tanner, C.B. and Pelton, W.L., 1960. Potential evapotranspiration estimates by the approximate energy balance method of Penman. *J. Geophys. Res.*, 65: 3391–3413.
- Thom, A.S., 1975. Momentum, mass and heat exchange of plant communities. p. 57–109. In: J.L. Monteith (Editor), *Vegetation and the Atmosphere*. Academic Press, New York, pp. 57–109.
- Wooding, R.A., Bradley, E.F. and Marshall, J.K., 1973. Drag due to regular arrays of roughness elements of varying geometry. *Boundary-Layer Meteorol.*, 5: 285–308.